Macromolecules
ARTICLE

*Macromolecules* **2010**, *43*, 9613–9619 **9613**
DOI: 10.1021/ma102157e

# Optically Active Helical Polyacetylene@silica Hybrid Organic−inorganic Core/Shell Nanoparticles: Preparation and Application for Enantioselective Crystallization

**Bo Chen,[†,‡] Jianping Deng,*[,†,‡] Linyue Tong,[†,‡] and Wantai Yang[†,‡]**

[†]*State Key Laboratory of Chemical Resource Engineering, Beijing University of Chemical Technology, Beijing 100029, China, and* [‡]*College of Materials Science and Engineering, Beijing University of Chemical Technology, Beijing 100029, China*

*Received September 16, 2010; Revised Manuscript Received October 18, 2010*

ABSTRACT: This article reports on a novel category of hybrid nanoparticles (NPs) consisting of a unique organic core (composed of optically active helical polyacetylene) and an inorganic shell (composed of silica). The NPs were synthesized by combining in one system the aqueous catalytic microemulsion polymerization of substituted acetylene monomer to form the core and the sol−gel approach of TEOS to form the shell. The substituted polyacetylene forming the core adopted helical conformations of predominant one handedness while the silica shell provided desirable protection for the core. The obtained emulsions exhibited high stability. The NPs possessed large optical activities, arising from the helical polymer chains constituting the core. The investigations are important in chemistry since two diverse research fields (organic helical polymers and inorganic materials) were combined for the first time in a specific system. The obtained hybrid core/shell NPs induced enantioselective crystallization of alanine enantiomers, attesting to the potential applications of the novel core/shell NPs.

## Introduction

Hybrid materials consisting of organic and inorganic building blocks are gathering ever-increasing attention because of the combination of superior properties not possessed by the individual components.[1] In such advanced hybrid materials, of particular interest should be core/shell structured nanoparticles (NPs).[2] For preparing core/shell architectures, silica may be the most popular inorganic material for shell due to its protection of the core from aggregation and the attacks from the environment[3] and also due to its wide practical uses for instance in separation,[4] biotechnology and medicine,[5] chemosensors,[6] and coatings.[7] The silica shells provide additional benefit of facilitating biocompatibility and biofunctionalization.[8] The core materials in organic−inorganic core/shell NPs can be a dye,[9] fluorescent conjugated polymer[10] and co- or terpolymer,[11] etc. However, to the best of our knowledge, there have been no organic−inorganic hybrid core/shell NPs derived from a synthetic optically active helical polymer yet, despite a great number of artificial helical polymers reported in literature.[12]

For some conjugated polymers including polyaniline,[13] polypyrrole,[14] and polythiophene,[15] many reports can be found in literature devoted to their core/shell NPs, but for acetylene and derivatives, only one paper was found most recently from us reporting acetylene-based core/shell NPs.[16] The Mecking group also have made breakthroughs in preparing acetylene-based NPs.[17] In our earlier study, a series of polymeric NPs were obtained by catalytic emulsion polymerizations of substituted acetylenes in aqueous systems.[18] More interestingly, by combining such a catalytic emulsion polymerizations and a free radical polymerization of methyl methacrylate (MMA) in a single aqueous system, a unique category of core/shell NPs were successfully prepared,[16] where the core is made up of helical polyacetylenes and the shell is made up of PMMA. The substituted polyacetylene cores in these NPs adopted ordered helical structures. A further combination of the aqueous catalytic emulsion polymerization of a substituted acetylene and a sol−gel technique forming silica[19] will in theory result in an unprecedent category of organic−inorganic hybrid core/shell NPs: the core comprising helical substituted polyacetylenes and the shell consisting of silica. Fortunately, we succeeded in preparing such interesting NPs. This article reports this novel type of hybrid core/shell NPs possessing unique structural features and showing large optical activities. Taking into consideration of the inherent undesirable heat- and oxygen-sensitivity of especially monosubstituted polyacetylenes, the unprecedent fabrication of core/shell NPs is indeed of great significance in chemical field, since the disadvantages mentioned above might be successfully circumvented through the encapsulation of the polyacetylene-based cores by protective silica shells.

After the success in preparing the hybrid core/shell NPs, we further employed them for enantioselective crystallization of amino acid enantiomers, on the basis of our earlier studies on the chiral recognition/chiral resolution performances of optically active helical substituted polyacetylenes.[20] Herein, alanine enantiomers were used as model chiral compounds to be separated. The novel core/shell NPs were found to induce preferential crystallization of one enantiomer of the two alanine chiral forms, demonstrating the significant potential applications of this type of hybrid core/shell NPs in chiral resolution, a significant field of extensive interest to both scientific research and practical applications. As far as enantioselective crystallization is concerned, large progress has been achieved.[21] For instance, Mastai group[22] used chiral polymers, macrospheres, emulsions, films, etc. for preferential crystallization and has made great contribution to the advancement in this field. However, no report has been found

*Corresponding author. Telephone: +86-10-6443-5128. Fax: +86-10-6443-5128. E-mail: dengjp@mail.buct.edu.cn.



Published on Web 11/11/2010

yet to induce preferential crystallization by using core/shell NPs made up of optically active helical polymers.

## Experimental Section

**Materials.** Solvents were distilled under reduced pressure. Freshly deionized water was used for polymerizations. Propargylamine, 1*S*-(+)-10-camphorsulfonyl chloride, and 1*R*-(−)-10-camphorsulfonyl chlorid were purchased from Aldrich and used as received without further purification. (nbd)$Rh^+B^-(C_6H_5)_4$ was prepared as reported.[25] TEOS (tetraethyl orthosilicate), Triton X-100 (poly(ethylene glycol) tert-octylphenyl ether) and HF acid (hydrofluoric acid) were bought from Aldrich and directly used. D- and L-Alanine purchased from Aldrich were used as received. All the other reagents were directly used without purification.

**Measurements.** Circular dichroism (CD) and UV−vis absorption spectroscopy measurements were conducted on a Jasco 810 spectropolarimeter. The molecular weights and molecular weight polydispersities were determined by GPC (Shodex KF-850 column) calibrated by using polystyrenes, with THF as eluent. Transmission electron microscopy (TEM) and scanning electron microscopy (SEM) were performed on the polymer and PSA−silica core/shell nanoparticle emulsions with Hitachi H-800 and Hitachi S-4700 electron microscope. Before carrying out the TEM experiments, the emulsions were first diluted. The *cis* content of the substituted polyacetylenes were determined by Raman spectroscopy. Specific rotations were measured on a JASCO P-1020 digital polarimeter with a sodium lamp as the light source at room temperature by using the emulsion without dilution. X-ray diffraction (XRD) analysis was performed on the crystals of D- and L-alanine with Shimadzu XRD-6000.

**Synthesis of PSA−Silica Core/Shell Nanoparticles.** The substituted acetylene monomers (SA; the polymer prepared from SA is defined as PSA) were synthesized according to previous reports.[18a,23] The aqueous catalytic microemulsion polymerization was reported in detail earlier.[18a] The major procedure is as follows. Predetermined amounts of Triton X-100 (2.88 g, 4.5 mmol) and deionized water (approximately 17 mL) were added to a reactor. The aqueous solution was stirred with a stirring rate of 350 rpm for 15 min at 30 °C, after which the solution of SA (0.1 g, 0.37 mmol)/DMF (6.5 mL) was dropwise added to the solution above. The solution mixture was subsequently stirred for 10 min, in which the catalyst (0.002 g, 0.0037 mmol)/DMF (6.5 mL) solution was dropwise added. The polymerization of SA was performed under $N_2$ at 30 °C for 1.5 h. With the polymer emulsion prepared above as the seeded emulsion, a predetermined amount of TEOS was dropwise added to the emulsion with a stirring rate of 350 rpm for 4 h at 30 °C and then the hydrolysis−condensation reaction happened. The other processes were the same as those for the preparation of core/shell particles with vinyl polymers as shells.[16]

In order to acquire pure substituted polyacetylene from the PSA−silica core/shell NPs, Triton X-100 was repeatedly excluded by centrifugation (centrifuge, GL-22MS, maximum speed, 22000 r/min) and a rotary evaporator was used to remove the water present in the emulsions above. Subsequently, HF acid (hydrofluoric acid, 0.25 M) was charged to the residual product and stirring was performed at room temperature for 5 min to exclude the silica shells. This process was repeated at least twice. The residual (*S*)-PSA and (*R*)-PSA were collected for the subsequent characterizations.

**Enantioselective Crystallization of Alanine.** All crystallization experiments were conducted from supersaturated aqueous solutions of alanine at room temperature. A typical procedure is as follows. D- and L-Alanine (270 mg, individually) were dissolved in 3 mL of deionized water, and the solution was heated to 35 °C. After complete dissolution, a predetermined amount of the chiral core/shell NPs prepared above was put into the racemic D- and L-alanine supersaturated solution and stirred for about 15 min. The solution was left to cool spontaneously to room temperature (approximately 25 °C). Crystals appeared in the solution and were filtrated after crystallization for 72 h. The crystal products were subject to XRD and CD spectroscopy analysis and the residual filtrate was subject to optical rotation measurements.

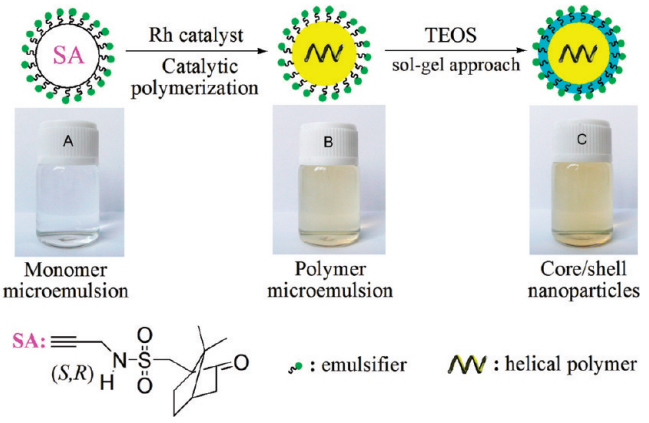


**Figure 1.** Schematic illustration of the strategy for the preparation of core/shell NPs: core = optically active helical poly(*N*-propargylsulfamide); shell = silica. A−C are the pictures for the emulsions: (A) monomer SA, (B) polymer of SA (PSA), and (C) core/shell NPs.

## Results and Discussion

**Strategy for the Preparation of PSA−Silica Core/Shell NPs.** The strategy for preparing the expected helical polyacetylene-silica core/shell NPs is schematically outlined in Figure 1. Such intriguing core/shell NPs were formed via a facile, straightforward one-pot two-stage procedure. In the first step, the helical substituted polyacetylene (core) was preformed via an aqueous catalytic microemulsion polymerization, and in a second step, the shells were formed via a sol−gel approach of TEOS (tetraethyl orthosilicate) in the same aqueous system, as described in Figure 1. The as-prepared NPs showed high stability attributed to the protection offered by the robust silica shell. These NPs also exhibited large optical activities resulting from the substituted polyacetylene adopting ordered helical structures with one preferential chirality. More details will be introduced later on.

*Morphology of PSA−Silica Core/Shell Nanoparticles.* Herein, for the purpose of conciseness in the following discussion, the polymers from *N*-propargyl-(1*S*)-camphor-10-sulfamide [(*S*)-SA] and *N*-propargyl-(1*R*)-camphor-10-sulfamide [(*R*)-SA] are defined as (*S*)-PSA and (*R*)-PSA, respectively. In Figure 1, take monomer (*S*)-SA as an example, the monomer first formed a clear aqueous emulsion in the presence of Triton X-100 (Figure 1, A). Stable latex particles of (*S*)-PSA were obtained next via aqueous catalytic microemulsion polymerization of SA with a Rh-based catalyst [(nbd)$Rh^+B^-(C_6H_5)_4$]. The involved aqueous catalytic microemulsion polymerization was investigated in detail earlier.[18] Finally TEOS of a predetermined amount was added into the above latex system at room temperature to prepare the shells via the sol−gel approach. In the step of forming silica shells, the hydrophobic TEOS should be distributed inside the preformed micelles and predominanttly adsorbed on the outer surface of the (*S*)-PSA core particles stabilized by Triton X-100 surfactant molecules, as schematically displayed in Figure 1. As a consequence, TEOS ended up as a shell on the surface of the (*S*)-PSA core particles, and eventually silica shells were formed via hydrolysis−condensation reaction of TEOS. The occurrence of this

reaction was preliminarily supported by the FT-IR spectra analysis (Figure 2), where the vibrational absorption peaks at 3281, 1324, 1088, and 815 $cm^{-1}$ can be assigned to $\nu$NH, $\nu$a, $SO_2$, $\nu$SiO and $\nu$a,SiO, respectively. The formation of silica shell can be further evidently confirmed by the TEM images of the obtained NPs, as presented in Figure 3 and Figure S1 (in Supporting Information; more clear TEM images of NPs) and will be discussed below.

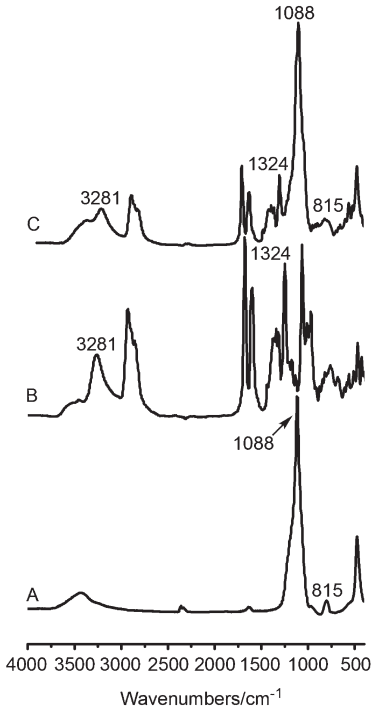


**Figure 2.** FT-IR spectra of (A) pure silica, (B) pure PSA NPs and (C) the PSA−silica core/shell NPs. All spectra were measured at room temperature (KBr tablet).

The obtained (*S*)-PSA−silica core/shell NPs emulsions were quite stable for at least a half year, well exemplified by the photographs in Figure 1C (SA/TEOS = 1/2.5, mol/mol). The pictures of the monomer (*S*)-SA emulsion before polymerization (Figure 1A) and the (*S*)-PSA emulsion (Figure 1B) are also presented together for a visual comparison. The addition of TEOS led to little change in the transparence of the emulsions, and the pale yellow color of the emulsions became a little darker with an increase in TEOS content due to the particles growing larger from pure (*S*)-PSA cores to core/shell NPs[18a,16] (see below). The average diameter of the original (*S*)-PSA NPs was approximately 90 nm (Figure 3A). Figure 3B−D presents the TEM images of the resulting core/shell NPs, in which the (*S*)-SA/TEOS ratio was 1/1, 1/2.5, and 1/5 (mol/mol), respectively. In all the core/shell NPs, the shells can be clearly distinguished from the cores. By increasing the content of TEOS, the shell thickness increased from 9.7 to 29.6 nm and then to 46.8 nm for the systems with (*S*)-SA/TEOS being 1/1, 1/2.5, and 1/5 (mol/mol), respectively. The relevant data are summarized in Table 1. It is thus demonstrated that the shell thickness can be easily controlled just by varying the amount of TEOS.

*Optical activities of PSA−Silica Core/Shell NPs Emulsions*. According to our preceding investigations, PSA could adopt helical structures both in solution[23] and in emulsion[16,18] and thus exhibited strong optical activities. Moreover, circular dichroism (CD) and UV−vis absorption spectroscopies have been proved effective and straightforward to identify the helical conformations of substituted polyacetylenes.[24] The present PSA−silica core/shell NPs emulsions were also analyzed by CD and UV−vis absorption spectroscopy measurements. The obtained CD spectra are illustrated in Figure 4A. Herein CD spectra of the core/shell NPs with (*S*)-SA/TEOS being 1/1, 1/2.5, and 1/5 (mol/mol) can be

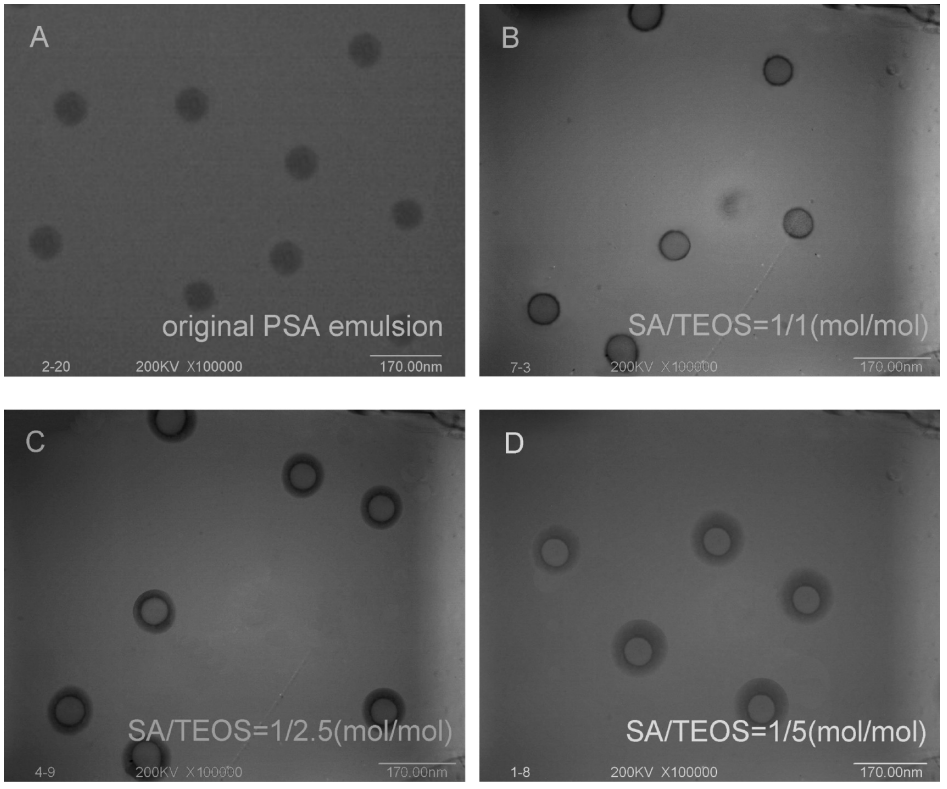


**Figure 3.** TEM images of (A) the pure PSA NPs and (B-D) the PSA−silica core/shell NPs with varied SA/TEOS ratios.

directly measured without any dilution of the emulsions due to their high transparence. CD signals can be clearly observed around 300 nm (304 nm), just like the original (*S*)-PSA emulsion (299 nm)[18] and the PSA/PMMA core/shell NPs emulsion (298 nm).[16] The CD signals around 300 nm in all the three NPs emulsions (SA/TEOS = 1/1, 1/2.5, 1/5 in mol/mol)) almost kept the same along with the increase in the TEOS concentration, as seen in Figure 4A. Nevertheless, the CD signal intensity of the (*S*)-PSA−silica core/shell NPs emulsions showed a slight decrease (from 250 to approximately 180 mdeg) when compared to that of the pure (*S*)-PSA emulsion. This phenomenon was also observed in PSA/PMMA core/shell NPs emulsions.[16] A comparison among the CD spectra of the present (*S*)-PSA−silica core/shell NPs emulsions with those of the pure (*S*)-PSA NPs emulsion and (*S*)−PSA-PMMA core/shell NPs emulsions demonstrated that the (*S*)-PSA−silica core/shell NPs emulsions also possessed large optical activities. This consideration is also evidenced by the optical rotations in Table 1. By referring to our earlier studies, the large optical activity observed in the present core/shell NPs was originated in the core-forming PSA which adopted helical structures with a preferential helicity.

**Table 1. Data of the PSA Particles and the PSA−Silica Core/Shell Structured NPs**

| | | diameter (thickness)(nm)[a] | | optical activity | |
|---|---|---|---|---|---|
| particles | SA/TEOS (mol/mol) | core | shell | $[\theta]$ (mdeg)[b] | $[\alpha]_D$ (deg)[c] |
| PSA | 1/0 | 90.4 | | 251.1 | 849 |
| PSA−silica core/shell | 1/1 | 91.2 | 9.7 | 181.1 | 791 |
| | 1/2.5 | 90.8 | 29.6 | 180.2 | 819 |
| | 1/5 | 92.1 | 46.8 | 179.7 | 801 |

[a] Determined according to TEM images. [b] According to the CD spectra in Figure 3. [c] Measured by polarimeter under the same conditions by using emulsions without dilution.

The UV−vis absorption spectra of the emulsions showed UV absorptions at a wavelength range from ca. 290−410 nm, as presented in Figure S2 (in the Supporting Information). To make the spectra more detailed, the core/shell NPs emulsions were diluted with water to varying times (emulsion/$H_2O$ = 1/5, 1/10, 1/20, and 1/40, mL/mL) and the recorded spectra are illustrated in Figure S3 (in the Supporting Information), in which the CD signal intensities at about 300 nm gradually decreased with the addition of water. This is also true for the UV−vis absorptions. The decrease in both CD signal and UV−vis absorption intensities while diluting the emulsions were in good agreement with the observations in our earlier pure PSA[18] and PSA−PMMA core/shell NPs.[16] In a control measurement, the CD and UV−vis absorption spectra of silica prepared under the same conditions but without SA (Figure S4 in the Supporting Information) showed negligible CD effect in the examined wavelength range (200−500 nm) and no considerable UV−vis absorption peak at wavelength over 275 nm. According to the investigations above and referring to our earlier investigations,[16,18,23] it is further concluded that the PSA chains in the core adopted helical conformations with a predominant screw sense.

*Stability of the NPs.* PSA synthesized by traditional solution polymerization will lose its helical structures by approximately 1/3 when the temperature was increased from −50 to +50 °C.[23] For the present (*S*)-PSA−silica core/shell NPs emulsions, the CD spectra (Figure 4B) exhibited little difference even when the temperature was elevated from 25 °C up

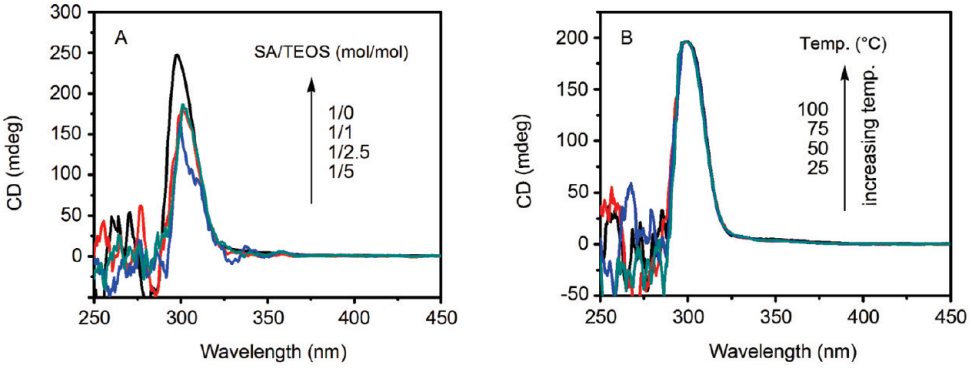


**Figure 4.** CD spectra of (A) the pure PSA emusion and the core/shell NPs emulsions with varied SA/TEOS ratios recorded at room temperature and (B) the core/shell NPs emulsion with SA/TEOS = 1/2.5 (mol/mol) at varied temperatures. The CD spectra were recorded by using the emulsions without dilution.

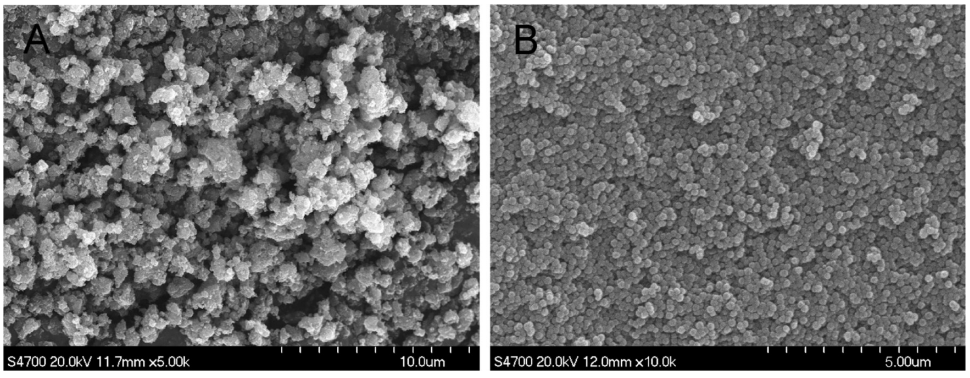


**Figure 5.** Typical SEM images of (A) PSA NPs and (B) PSA−silica core/shell NPs (for PSA−silica core/shell NPs, SA/TEOS = 1/5, mol/mol).

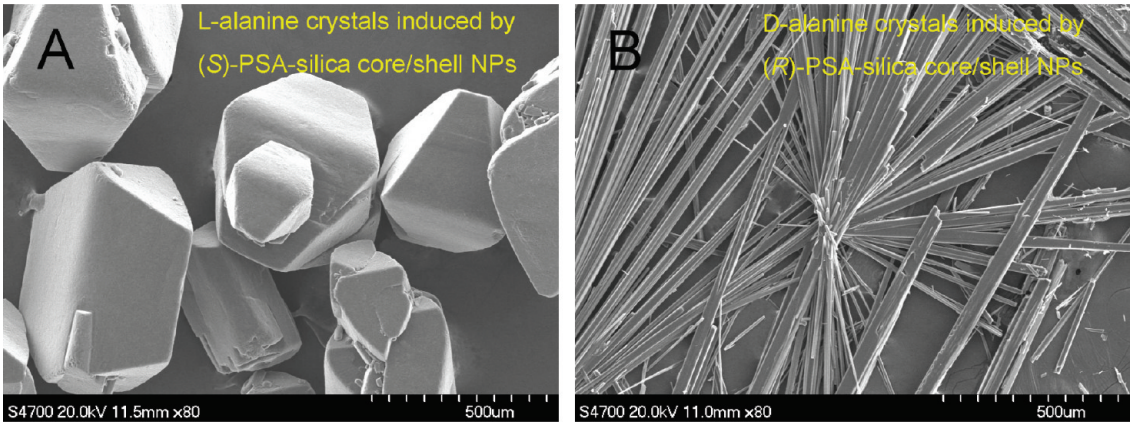


**Figure 6.** SEM images of crystals formed via enantioselective crystallization in racemic D- and L-alanine supersaturated solutions induced by (A) NPs consisting of (*S*)-PSA and (B) NPs consisting of (*R*)-PSA under the same experimental conditions. $T = 72$ h, $c = 1.98$ M; the solutions were left to cool spontaneously from 35 °C to room temperature (approximately 25 °C).

to 100 °C. This observation is also observed in the diluted NPs emulsions (Figure S5 in the Supporting Information). These phenomena indicated the high stability in the secondary structures of the substituted polyacetylene constituting the core of the NPs, resulting from the heat-insulating property of the silica shells. The $M_n$ and its $M_w/M_n$ of PSA in core/shell NPs heated at 50, 75, and 100 °C for 20 min were found to be 10100 and 1.51 (50 °C); 9980, 1.46 (75 °C); and 10000, 1.41 (100 °C), respectively, while before heating they were 9900 ($M_n$) and 1.48 ($M_w/M_n$) for the PSA in the core/shell NPs emulsion. Accordingly, it is demonstrated that little degradation occurred to the PSA core, and it is thus indicated that silica constituting the shell provided an excellent protection for the PSA inside the core/shell NPs. Meanwhile, the TEM images (Figure S6, Supporting Information) of heated (*S*)-PSA−silica core/shell NPs (SA/TEOS = 1/2.5, mol/mol, $t = 20$ min, $T = 100$ °C) showed little difference than the NPs before heat treatment (Figure 3C), also demonstrating the high stability of PSA−silica core/shell NPs.

In addition to providing the protection for PSA cores, the silica shells also enabled the PSA NPs to keep regular morphologies, desirable stability and dispersity, as evidenced in Figure 5. Figure 5A shows that the pristine (*S*)-PSA NPs tended to undergo considerable aggregation by themselves, while the core/shell NPs in Figure 5B remained round in shape and little aggregation occurred. Accordingly, the silica shells played multiple roles in the present core/shell NPs.

The shell (silica) and the core (PSA) of the prepared core/shell NPs were isolated to acquire deep insights into the novel particles. For this purpose, the silica shells were etched with HF acid at a moderate concentration, and then the core material PSA was collected for further analyses. Taking the specific system with (*S*)-SA/TEOS = 1/2.5 (mol/mol) as representative, the core-forming PSA was further investigated to explore the effects of the shell forming process and the existence of silica shell on PSA. It was found that the preformed PSA was hardly influenced by the inorganic silica shells according to the data on molecular weight and cis content of PSA. $M_n$, $M_w/M_n$, and the cis content of the original PSA were 9900, 1.48, and 98%, respectively, while they were 10200, 1.49, and 99%, respectively, for the PSA acquired from the core of the PSA−silica core/shell NPs. This demonstrates in evidence that silica shells had little influence on the preformed polyacetylene chains inside the shells.

The pure (*S*)-PSA particles before the formation of core/shell structures and after removing the shell were also compared. A TEM image is displayed in Figure S7 (in Supporting Information) for the latter. When a comparison was made between Figure S7 and Figure 3A, little difference can be seen in the two groups of (*S*)-PSA particles. It can be considered further that TEOS underwent reaction only on the surface of PSA core and that the shell-forming approach scarcely affected the helical polymers constituting the cores of final core/shell NPs. This conclusion was also evidenced by the investigations concerning $M_n$ and $M_w/M_n$ of the PSA core, as discussed above.

*Enantioselective Crystallization*. The pure PSA nanoparticles (i.e., the cores of the core/shell nanoparticles) were initially used to perform enantioselective crystallization of amino acids. However, due to the severe aggregation among the PSA nanoparticles, as presented in Figure 5A, the results of enantioselective crystallization was not satisfactory. On the other hand, since the hybrid core/shell NPs consist of cores made up of optically active helical polymer chains and show large optical activities, each nanoparticle can be considered as a bulk "chiral" entity, and may also act as nucleation sites for inducing preferential crystallizataion of one chiral enantiomer. This hypothesis was proved true by our investigations. The crystallization experiments were performed at room temperature in the presence of NPs, taking racemic D,L-alanine as a model. We found that D- and L-enantiomer of alanine preferentially crystallized on the corresponding core/shell NPs: D-alanine preferentially crystallized on (*R*)-PSA-based NPs, while L-alanine crystallized on (*S*)-PSA-based NPs. Morphology of the resulting D- and L-alanine crystals were collected and observed by SEM. The obtained images are presented in Figure 6, parts A and B.

In Figure 6A, L-alanine crystals showed octahedral structures, while in the case of D-alanine, needle-like crystals can be clearly observed in Figure 6B. Furthermore, the obtained crystals are highly regular and pure. Namely, almost only one crystal structure appeared in each case. The seeded core/shell NPs were encapsulated completely by the crystals, providing an evidence for the consideration that such NPs acted as nucleation sites for inducing the formation of crystals. Such crystals seem to be in well agreement with the corresponding pure L- and D-alanine emantiomer crystals (Figure S8 in the Supporting Information). The crystalls were further subjected to XRD analyses, and the obtained spectra are illustrated in Figure S9 (Supporting Information), taking L-alanine as the representative. The two spectra are almost entirely the same for the two crystals, even one from pure L-alanine enantiomer and the other from L-alanine prepared

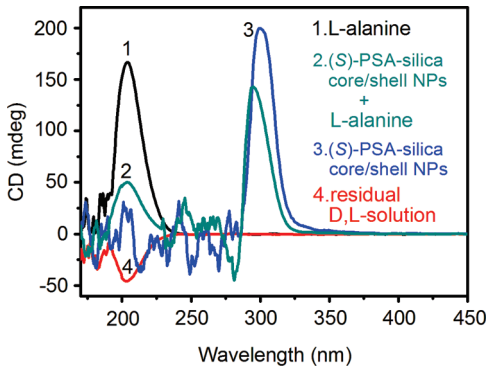


**Figure 7.** CD spectra of the crystals obtained via enantioselective crystallization [(*S*)-PSA core/shell NPs + L-alanine], (*S*)-core/shell NPs, L-alanine, and the residual racemic alanine solutions (crystallization for 60 h).

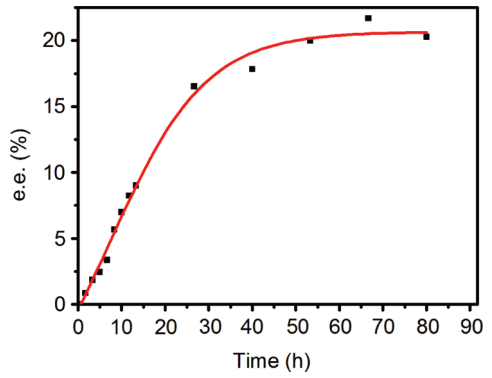


**Figure 8.** e.e. (%) as a function of crystalliation time (L-alanine in excess) of 15 mL racemic alanine supersaturated solutions (*R*-alanine/L-alanine = 1325/1325, in mg), 2.5 mg of chiral (*S*)-PSA−silica core/shell NPs.

via enantioselective crystallization. It should be pointed out that, the crystal structures of L- and D-alanine emantiomers are quite differet in morphology, as demonstrated in Figure 6. Similar phenomena were reported in literature,[26] i.e., the same alanine show different crystal morphologies when prepared under varied conditions.

After crystallization, L-alanine crystals obtained from racemic D- and L-alanine solution, together with core/shell NPs from (*S*)-PSA, were subjected to CD spectroscopy measurement. The spectra are shown in Figure 7. The CD spectrum of the residual racemic alanine aqueous solution was also presented there. When compared to pure L-alanine and pure core/shell NPs, the L-alanine obtained via enantioselective crystallization (together with the core/shell NPs from (*S*)-PSA) showed the CD signals of both L-alanine and (*S*)-PSA. This observation is consistent with the results of enantioselective crystallization discussed above. The chiral separation efficiency of core/shell NPs consisting of (*S*)-PSA was further determined by measuring the optical rotation ($\alpha$) of the residual racemic alanine solution. Figure 8 shows the relevant results. A maximum e.e. value of 23.4% was achieved after 68 h of enantioselective crystallization. Even though the present e.e. values are not high enough from a viewpoint of practial applications, the novel type of hybrid core/shell NPs definitely showed significant potential applications in chiral resolution. Investigations are currently in progress along this direction. We are also convinced that high e.e. values will be achieved by optimizing the structures and compositions of the optically active core/shell NPs.

## Conclusions

We have prepared a novel category of core/shell structured NPs according to a strategy of general applicability. The cores comprise helical substituted polyacetylene while the shells consist of inorganic silica. The as-prepared core/shell NPs combine the advantages of the two components in one single system: the large optical activity from the helical polymer core and the high stability from the inorganic silica shell. Therefore, the present core/shell NPs well bridged the two significant research fields, i.e., organic helical polymers and inorganic silica. It is convinced that, taking the present strategy and novel core/shell NPs as a platform, a series of highly functional NPs will be prepared next by selecting the suited organic and inorganic materials and by controlling the detailed structures and morphology of the NPs. More importantly, the prepared hybrid core/shell NPs demonstrated the exciting utility for enantioselective crystallization of amino acid enantiomers. Further investigations will focus on optimizing the chiral core/shell NPs and improving the chiral separation efficiency.

**Acknowledgment.** This work is supported by the "Program for New Century Excellent Talents in University" (NCET-06-0096), the "National Science Foundation of China" (20974007), "Program for Changjiang Scholars and Innovative Research Team in University" (PCSIRT, IRT0706), the "Project of Polymer Chemistry and Physics, Beijing Municipal Commission of Education", and the "Innovation Funds for Outstanding Doctoral Dissertation of BUCT."

**Supporting Information Available:** Figures showing UV−vis and CD spectra of PSA and PSA-core/silica-shell NPs, TEM images of core/shell NPs, XRD spectra of L-alanine crystals and SEM images of pure D-and L-alanine crystals. This material is available free of charge via the Internet at http://pubs.acs.org.

## References and Notes

(1) (a) Landfester, K. *Angew. Chem., Int. Ed.* **2009**, *48*, 4488. (b) Guerrero-Martínez, A.; Pérez-Juste, J.; M. Liz-Marzán, L. *Adv. Mater.* **2010**, *22*, 1182. (c) Corma, A.; Díaz, U.; Arrica, M.; Fernández, E.; Ortega, I. *Angew. Chem., Int. Ed.* **2009**, *48*, 6247. (d) Jin, Y.; Li, A.; Hazelton, S. G.; Liang, S.; John, C. L.; Selid, P. D.; Pierce, D. T.; Zhao, J. X. J. *Coord. Chem. Rev.* **2009**, *253*, 2998. (e) Kuschel, A.; Sievers, H.; Polarz, S. *Angew. Chem., Int. Ed.* **2008**, *47*, 9513. (f) Hoffmann, F.; Cornelius, M.; Morell, J.; Froba, M. *Angew. Chem., Int. Ed.* **2006**, *45*, 3216. (g) Kickelbick, G. *Prog. Polym. Sci.* **2003**, *28*, 83. (h) Kwak, G.; Kim, S. -Y.; Fujiki, M.; Masuda, T.; Kawakami, Y.; Aoki, T. *Chem. Mater.* **2004**, *16*, 1864.

(2) (a) Tang, J.; Zhou, X.; Zhao, D.; Lu, Q. G.; Zou, J.; Yu, C. *J. Am. Chem. Soc.* **2007**, *129*, 9044. (b) Yuan, J. J.; Mykhaylyk, O. O.; Ryan, A. J.; Armes, S. P. *J. Am. Chem. Soc.* **2007**, *129*, 1717. (c) Sertchook, H.; Elimelech, H.; Makarov, C.; Khalfin, R.; Cohen, Y.; Shuster, M.; Babonneau, F.; Avnir, D. *J. Am. Chem. Soc.* **2007**, *129*, 98. (d) Huo, Q.; Liu, J.; Wang, L. Q.; Jiang, Y.; Lambert, T. N.; Fang, E. *J. Am. Chem. Soc.* **2006**, *128*, 6447. (e) Caruso, F. *Adv. Mater.* **2006**, *18*, 795. (f) Jang, J.; Lim, B. *Angew. Chem., Int. Ed.* **2003**, *42*, 5600. (g) Cardin, D. J. *Adv. Mater.* **2002**, *14*, 553.

(3) (a) Salgueiriño-Maceira, V. S.; Spasova, M.; Farle, M. *Adv. Funct. Mater.* **2005**, *15*, 1036. (b) Graff, C.; Vossen, D. L. J.; Imhof, A.; Van Blaaderen, A. *Langmuir* **2003**, *19*, 6693. (c) Kobayashi, Y.; Horie, M.; Konno, M.; Rodríguez-González, B.; Liz-Marzán, L. M. *J. Phys. Chem. B* **2003**, *107*, 7420.

(4) (a) Pesek, J. J.; Matyska, M. T. J. *Sep. Sci.* **2009**, *32*, 3999. (b) Bamba, T.; Fukusaki, E. J. *Sep. Sci.* **2009**, *32*, 2699.

(5) (a) Pasqua, L.; Cundari, S.; Ceresa, C.; Cavaletti, G. *Curr. Med. Chem.* **2009**, *16*, 3054. (b) Wang, L.; Zhao, W.; Tan, W. *Nano Res.* **2008**, *1*, 99.

(6) Han, W. S.; Lee, H. Y.; Jung, S. H.; Lee, S. J.; Jung, J. H. *Chem. Soc. Rev.* **2009**, *38*, 1904.

(7) Pagliaro, M.; Ciriminna, R.; Palmisano, G. J. *Mater. Chem.* **2009**, *19*, 3116.

(8) (a) Knopp, D.; Tang, D.; Niessner, R. *Anal. Chem. Acta* **2009** *647*, 14. (b) Webster, A.; Compton, S. J.; Aylott, J. W. *Analyst* **2005**, *130*, 163.
(9) Sathiyamoorthy, K.; Vijayan, C.; Varma, S. *Langmuir* **2008**, *24*, 7485.
(10) (a) Burns, A.; Sengupta, P.; Zedayko, T.; Baird, B.; Wiesner, U. *Small* **2006**, *2*, 723. (b) Wu, C.; Szymanski, C.; McNeill, J. *Langmuir* **2006**, *22*, 2956.
(11) (a) Wang, J.; Yang, X. *Colloid Polym. Sci.* **2008**, *286*, 283. (b) Armini, S.; Vakarelski, I. U.; Whelan, C. M.; Maex, K.; Higashitani, K. *Langmuir* **2007**, *23*, 2007.
(12) (a) Yashima, E.; Maeda, K.; Iika, H.; Furusho, Y.; Nagai, K. *Chem. Rev.* **2009**, *109*, 6102. (b) Rudick, J. G.; Percec, V. *Acc. Chem. Res.* **2008**, *41*, 1641. (c) Fujiki, M. *Top. Curr. Chem.* **2008**, *284*, 119. (d) Masuda, T. *J. Polym. Sci., Part A: Polym. Chem.* **2007**, *45*, 165. (e) Lam, J. E. Y.; Tang, B. Z. *Acc. Chem. Res.* **2005**, *38*, 745. (f) Aoki, T.; Kaneko, T.; Maruyama, N.; Sumi, A.; Takahashi, M.; Sato, T.; Teraguchi, M. *J. Am. Chem. Soc.* **2003**, *125*, 6346. (g) Nakano, T.; Okamoto, Y. *Chem. Rev.* **2001**, *101*, 4013. (h) Ky Hirschberg, J. H. K.; Brunsveld, L.; Ramzi, A.; Jef Vekemans, A. J. M.; Sijbesma, R. P.; Meijer, E. W. *Nature* **2000**, *407*, 167. (i) Novak, B. M. *J. Am. Chem. Soc.* **2004**, *126*, 3722. (j) Green, M. M.; Park, J. W.; Sato, T.; Teramoto, A.; Lifson, S.; Selinger, R. L. B.; Selinger, J. V. *Angew. Chem., Int. Ed.* **1999**, *38*, 3138.
(13) (a) Lee, H.-Y.; Rwei, S.-P.; Wang, L.; Chen, P.-H. *Mater. Chem. Phys.* **2008**, *112*, 805. (b) O'Mullane, A. P.; Dale, S. E.; Macpherson, J. V.; Unwin, P. R. *Chem. Commun.* **2004**, 1606. (c) Niu, Z.; Yang, Z.; Hu, Z.; Lu, Y.; Han, C. C. *Adv. Funct. Mater.* **2003**, *13*, 949.
(14) (a) Wang, J.; Sun, L.; Mpoukouvalas, K.; Lienkamp, K.; Lieberwirth, I.; Fassbender, B.; Bonaccurso, E.; Brunklaus, G.; Muehlebach, A.; Beierlein, T.; Tilch, R.; Butt, H. -J.; Wegner, G. *Adv. Mater.* **2009**, *21*, 1137. (b) Xing, S.; Tan, L. H.; Chen, T.; Yang, Y.; Chen, H. *Chem. Commun.* **2009**, 1653. (c) Mangeney, C.; Fertani, M.; Bousalem, S.; Ma, Z.; Ammar, S.; Herbst, F.; Beaunier, P.; Elaissari, A.; Chehimi, M. M. *Langmuir* **2007**, *23*, 10940.
(15) (a) Hong, J. -Y.; Kwon, E.; Jang, J. *Soft Matter* **2009**, *5*, 951. (b) Zhang, Z.; Wang, F.; Chen, F.; Shi, G. *Mater. Lett.* **2006**, *60*, 1039.
(16) Chen, B.; Deng, J. P.; Yang, W. T. *Macromolecules* **2010**, *43*, 3177.
(17) (a) Huber, J.; Mecking, S. *Angew. Chem., Int. Ed.* **2006**, *45*, 6314. (b) Mecking, S. *Colloid Polym. Sci.* **2007**, *285*, 605.
(18) (a) Deng, J. P.; Chen, B.; Luo, X. F.; Yang, W. T. *Macromolecules* **2009**, *42*, 933. (b) Luo, X. F.; Kang, N. W.; Li, L.; Deng, J. P.; Yang, W. T. *J. Polym. Sci., Part A: Polym. Chem.* **2010**, *48*, 1661.
(19) Stober, W.; Fink, A.; Bohn, E. *J. Colloid Interface Sci.* **1968**, *26*, 62.
(20) (a) Zhou, K.; Tong, L. Y.; Deng, J. P.; Yang, W. T. *J. Mater. Chem.* **2010**, *20*, 781. (b) Du, X. Y.; Liu, J. B.; Deng, J. P.; Yang, W. T. *Polym. Chem.* **2010**, *1*, 1030.
(21) (a) Kofi, T. S.; Heike, L.; Morgenstern, S. *Cryst. Growth Des.* **2009**, *9*, 2387. (b) Kofi, T. S.; Heike, L.; Liane, H.; Thomas, E. F.; Morgenstern, S. *Cryst. Growth Des.* **2008**, *8*, 3408. (c) Wu, J. C.; Chow, Y.; Li, R. J.; Carpenter, K. *Sep Purif. Technol.* **2007**, *53*, 144. (d) Nakanishi, T.; Banno, N.; Matsunaga, M.; Asahi, T.; Osaka, T. *Chem. Senses.* **2004**, *20*, 862. (e) Shosuke, K.; Kyoko, T. *Chem. Commun.* **2001**, 1980.
(22) (a) Mastai, Y. *Chem. Soc. Rev.* **2009**, *38*, 772. (b) Medina, D. D.; Goldshtein, J.; Margel, S.; Mastai, Y. *Adv.Funct.Mater.* **2007**, *17*, 944.
(23) Zhang, Z. G.; Deng, J. P.; Zhao, W. G.; Wang, J. M.; Yang, W. T. *J. Polym. Sci., Part A: Polym. Chem.* **2007**, *45*, 500.
(24) (a) Luo, X. F.; Li, L.; Deng, J. P.; Guo, T. T.; Yang, W. T. *Chem. Commun.* **2010**, 2745. (b) Ding, L.; Jiao, X. F.; Deng, J. P.; Zhao, W. G.; Yang, W. T. *Macromol. Rapid Commun.* **2009**, *30*, 120. (c) Terada, K.; Masua, T.; Sanda, F. *Macromolecules* **2009**, *42*, 913. (d) Deng, J. P.; Luo, X. F.; Zhao, W. G.; Yang, W. T. *J. Polym. Sci., Part A: Polym. Chem.* **2008**, *46*, 4112.
(25) Schrock, R. R.; Osborn, J. A. *Inorg. Chem.* **1970**, *9*, 2339.
(26) (a) Lee, A. Y.; Ulman, A.; Myerson, A. S. *Langmuir* **2002**, *18*, 5886. (b) Ma, Y.; Cölfen, H.; Antonietti, M. *J. Phys. Chem. B* **2006**, *110*, 10822.